Inorganic Chemistry

ARTICLE

pubs.acs.org/IC

Synthesis of New Compound Gd_5Ni_{19} with a Superlattice Structure and Hydrogen Absorption Properties

Kenji Iwase,*[,†] Kazuhiro Mori,[‡] Akinori Hoshikawa,[†] and Toru Ishigaki[†]

[†]Frontier Research Center for Applied Atomic Sciences, Ibaraki University, 162-1 Shirakata, Tokai, Naka, Ibaraki 319-1106, Japan

[‡]Research Reactor Institute, Kyoto University, 2-1010 Asashiro-nishi, Kumatori, Sennan, Osaka 590-0494, Japan

ABSTRACT: We successfully synthesized the new intermetallic compound Gd_5Ni_{19} and determined its crystal structure by X-ray diffraction (XRD) and scanning transmission electron microscopy (STEM). The structure is a Sm_5Co_{19}-type superlattice structure (2H, space group $P6_3/mmc$), and the lattice parameters were determined as $a = 0.4950(1)$ nm and $c = 3.2161(5)$ nm by X-ray Rietveld refinement. The XRD results agreed with the STEM analysis results. The $P-C$ isotherm of Gd_5Ni_{19} was measured at 233 K. In the first absorption cycle, the maximum hydrogen capacity reached 1.07 H/M at 2.0 MPa. The sloping plateau was observed in the first absorption−desorption cycle. The maximum hydrogen capacity decreased by 0.87 H/M in the second absorption cycle, implying that hydrogen in the amount of H/M = 0.20 remained in the alloy before the second absorption−desorption cycle.

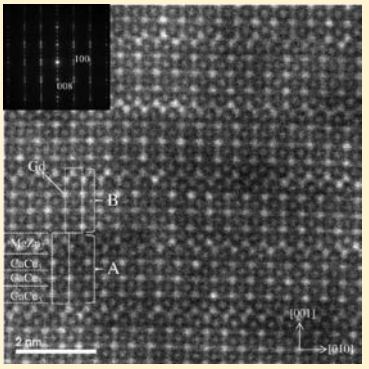

1. INTRODUCTION

Extensive studies have been conducted on the crystal structures of Gd−Ni binary compounds $GdNi_2$, $GdNi_3$, Gd_2Ni_7, and $GdNi_5$.[1−3] The Laves phase compound $GdNi_2$ has a cubic $MgCu_2$-type (C15) structure with lattice parameter $a = 0.72056$ nm.[1] $GdNi_3$ and Gd_2Ni_7 have superlattice structures and consist of cells with $MgZn_2$- and $CaCu_5$-type structures stacked along the c axis in ratios of 1:1 and 1:2, respectively. $GdNi_3$ has a hexagonal $PuNi_3$-type structure.[2] Gd_2Ni_7 has a hexagonal Ce_2Ni_7-type structure at low temperatures (873 K) and a rhombohedral Gd_2Co_7-type structure at high temperatures (1173 K).[3] $GdNi_5$ has a hexagonal $CaCu_5$-type structure.[4] The crystal structures of $LaNi_3$, La_2Ni_7, and $LaNi_5$ are isomorphic with $GdNi_3$, Gd_2Ni_7, and $GdNi_5$ compounds, respectively.

$GdNi_2$ has been investigated as a hydrogen-absorbing alloy.[5] The alloy is hydrogenated slowly with high-purity hydrogen gas (7 N) under 5 MPa; the alloy becomes amorphous after hydrogenation at 323 K and decomposes into GdH_2 and $GdNi_5$ after hydrogenation at 773 K. The $P-C$ isotherm of $GdNi_5$ was previously measured at a hydrogen gas pressure of 35 MPa.[6] The initial activation was achieved by exposing the alloy to a hydrogen gas pressure of 35 MPa at 197 K for several hours. The hydride showed two clear plateaus below 248 K. The lower and higher absorption plateaus were at 0.3 and 2.0 MPa, respectively, at 197 K. The maximum hydrogen capacity reached approximately 1.0 H/M at 197 K.

The crystal structures of intermetallic compound R_5Co_{19} (R = Ce, Pr, and Nd) were investigated by Khan.[7] Ce_5Co_{19} was determined to be rhombohedral (space group $R\bar{3}m$), and the lattice parameters were reported as $a = 0.4947$ (5) nm and $c = 4.8743$ (4) nm from X-ray diffraction (XRD) data. Pr_5Co_{19} was homogenized at 1173 K for 7−14 days, and the crystal structure agreed with that of Ce_5Co_{19}. The lattice parameters of Pr_5Co_{19} were $a = 0.506$ (5) nm and $c = 4.914$ (4) nm. Intermetallic compound La_5Ni_{19} was found for the first time by Yamamoto et al.[8] The crystal structure was determined to be of the Ce_5Co_{19} type (3R, space group $R\bar{3}m$) by transmission electron microscopy (TEM) analysis. The crystal structure of Sm_5Ni_{19} was found by Takeda et al. using TEM to be of the Sm_5Co_{19} type (2H, space group $P6_3/mmc$).[9] Ferey et al. reported that the crystal structure of La_5Ni_{19} was of the Sm_5Co_{19} type; they also measured its $P-C$ isotherm.[10] The lattice parameters of the alloy were $a = 0.50491(1)$ nm and $c = 3.2642$ (1) nm. The maximum hydrogen capacity reached 1.2 H/M. Lemort et al. reported the crystal structure and $P-C$ isotherm of Pr_5Ni_{19} and Nd_5Ni_{19}.[11] There have been only a few reports on R_5Ni_{19} compounds and their $P-C$ isotherms.

The structural change in $La_2Ni_7H_x$ with a superlattice structure was investigated using in situ XRD.[12] The crystal structures for the metal sublattice of the two hydride phases $La_2Ni_7H_{7.1}$ and $La_2Ni_7H_{10.8}$ were determined. The La_2Ni_4 and $LaNi_5$ cells of $La_2Ni_7H_{7.1}$ expanded by 48.9% and 6.0%, respectively, from the original alloy, and those of $La_2Ni_7H_{10.8}$ expanded by 69.8% and 12.2%, respectively. Most of the H atoms were located in the La_2Ni_4 cells.[13]

The phase diagram of the Gd−Ni system shows nine phases in the equilibrium state: Gd_3Ni_1, Gd_3Ni_2, GdNi, $GdNi_2$, $GdNi_3$, Gd_2Ni_7, $GdNi_4$, $GdNi_5$, and Gd_2Ni_{17}.[14] Gd_5Ni_{19} is not shown in the Gd−Ni binary phase diagram. This study focused on the

Received: July 21, 2011
Published: October 17, 2011

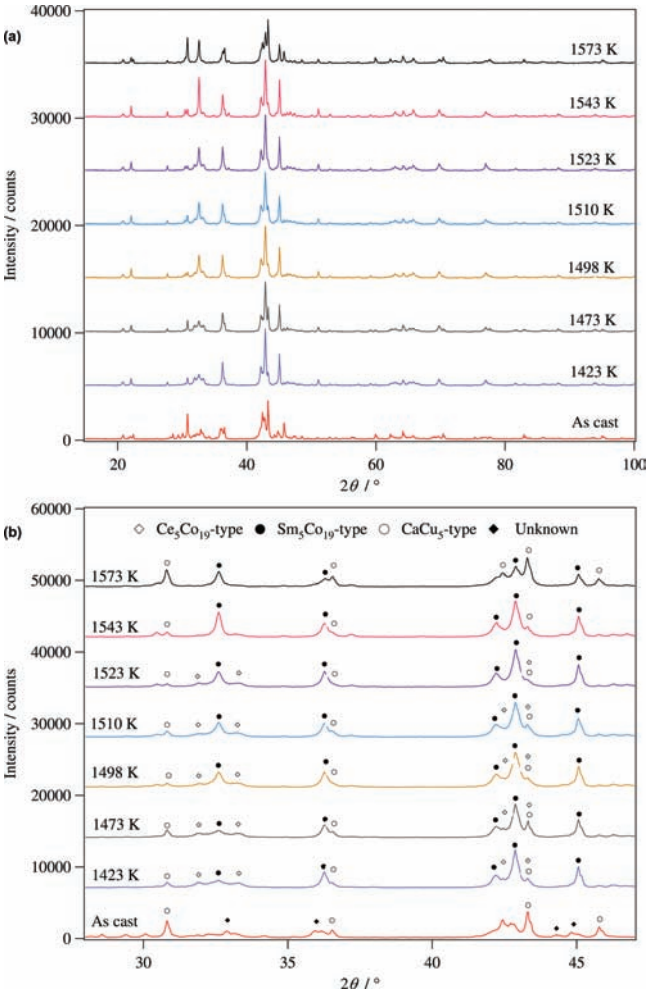

Figure 1. XRD profiles of the Gd_5Ni_{19} alloy as-cast and quenched from several temperatures: (a) 2θ region between 15° and 100°; (b) 2θ region between 28° and 47°.

crystal structure and $P-C$ isotherm of Gd_5Ni_{19}. We attempted to synthesize Gd_5Ni_{19} and determine the crystal structure by using XRD and scanning transmission electron microscopy (STEM). It is interesting to elucidate how the behavior of the $MgZn_2$- and $CaCu_5$-type cells is related to the hydrogenation properties. This paper presents the determined crystal structure and $P-C$ isotherm of Gd_5Ni_{19}.

2. EXPERIMENTAL SECTION

A Gd−Ni alloy was prepared by arc-melting Gd and Ni metals (99.9%) in an argon atmosphere. The obtained alloy ingot was annealed in the temperature region between 1423 and 1573 K under vacuum and then quenched in ice water.

The powder sample for XRD measurements was sieved to a particle size of <20 μm. The XRD data were collected by using the diffractometer Rigaku Ultima-IV in the step-scan mode. Cu Kα radiation monochromatized with a curved graphite diffractometer was used. The structural parameters were refined with the Rietveld refinement program *RIETAN-2000*.[15−17] The XRD data in the 2θ region between 15° and 100° were used for the Rietveld refinement. Data at the 2θ region around 33° contained a peak from an unknown phase and were excluded from the refinement. The reliability of the fitting was judged from the "goodness-of-fit" parameter S, which is defined as $S = R_{wp}/R_e$, where R_{wp} is a residue

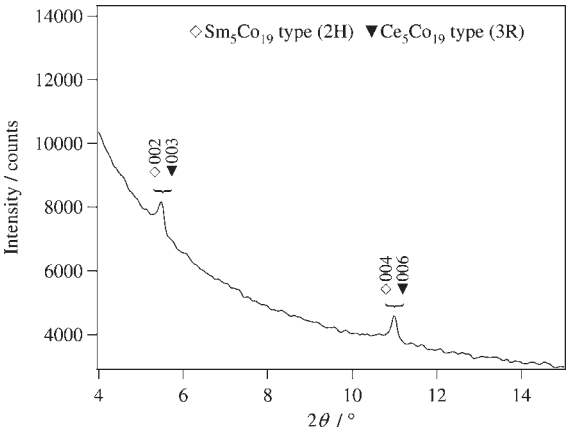

Figure 2. XRD profile of Gd_5Ni_{19} in a low-angle region. Two superlattice peaks corresponding to Sm_5Co_{19}-type (2H) or Ce_5Co_{19}-type (3R) structures were observed.

of the weighted pattern and R_e is the statistically expected residue. A JEOL JEM-2100F transmission electron microscope operating at 200 kV was used in the STEM observations.

The sample for the $P-C$ isotherm measurement was sealed in a stainless steel container heated in a vacuum at 413 K for 1 h and then kept at 233 K for 1 h. In the first cycle, the $P-C$ isotherm was measured by Sieverts' method with no other pretreatment for activation. Before the second cycle measurement, the sample was evacuated at 233 K for 3 h.

3. RESULTS

3.1. Crystal Structure of Gd_5Ni_{19}. XRD profiles of the quenched samples from several heat-treatment temperatures are shown in Figure 1a,b. The as-cast profile included the $CaCu_5$-type phase, and the peak broadening was observed. The Sm_5Co_{19}-type (2H), Ce_5Co_{19}-type (3R), and $CaCu_5$-type phases coexisted between 1423 and 1523 K. The Bragg peak intensity of the Ce_5Co_{19}-type structure decreased with increasing heat-treatment temperature and disappeared at 1543 K. The Bragg peak intensity of the $CaCu_5$-type structure increased and that of the Sm_5Co_{19}-type structure decreased when the temperature rose over 1573 K. Finally, the Gd_5Ni_{19} sample was obtained by annealing at 1543 K for 11.5 h under a vacuum of 2.0×10^{-2} Pa and quenching in ice water. The XRD profile of Gd_5Ni_{19} in the 2θ region between 4° and 15° is shown in Figure 2. Two superlattice reflections of the Sm_5Co_{19}-type structure (002 and 004) or Ce_5Co_{19}-type structure (003 and 006) were clearly observed. These peaks corresponded to d = 1.61 and 0.804 nm, respectively. The crystal structures of the Sm_5Co_{19} and Ce_5Co_{19} types are shown in Figure 3. The Sm_5Co_{19}-type structure has two blocks, A and B, along the c axis; each block is composed of one layer of $MgZn_2$-type cells and three layers of $CaCu_5$-type cells. The Ce_5Co_{19}-type structure has three blocks, A−C, along the c axis.

An initial structural model based on the Ce_5Co_{19}-type structure (space group $R\bar{3}m$) was adapted for Rietveld refinement. However, the calculated pattern did not fit well with the observed pattern. The goodness-of-fit S was as large as 5.5, indicating that the crystal structure of Gd_5Ni_{19} is not of the Ce_5Co_{19} type. The second structural model based on the Sm_5Co_{19}-type structure (space group $P6_3/mmc$) was then adapted. The calculated pattern fit well with the observation,

and S = 1.8. The final Rietveld refinement was carried out with a two-phase model containing Sm_5Co_{19}-type Gd_5Ni_{19} and $CaCu_5$-type $GdNi_5$, and the results are shown in Figure 4. The mass fractions of the Sm_5Co_{19}- and $CaCu_5$-type phases were 89% and 11%, respectively. The refined structural parameters of Sm_5Co_{19}-type Gd_5Ni_{19} are listed in Table 1.

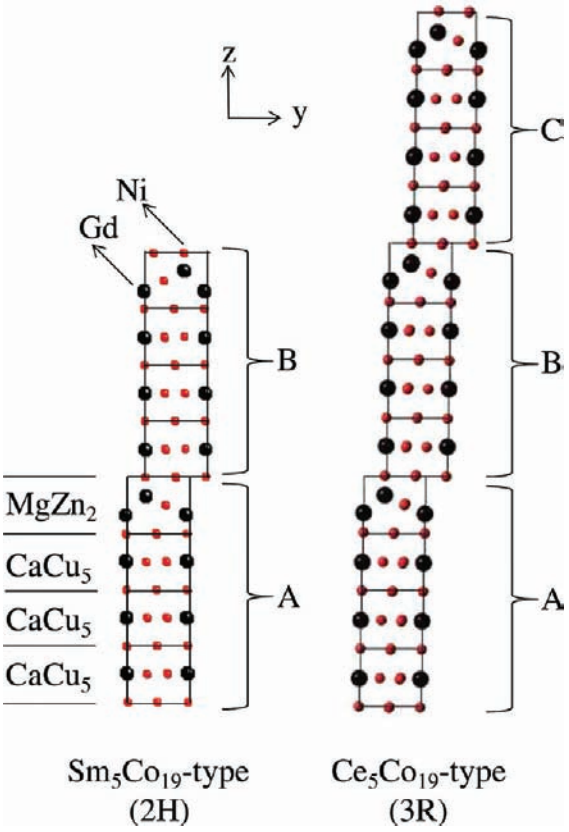

Figure 3. Sm_5Co_{19}-type (2H) and Ce_5Co_{19}-type (3R) structures, in which $MgZn_2$- and $CaCu_5$-type cells are stacked along the c axis.

$GdNi_4$ has a hexagonal structure with lattice parameters a = 0.535 nm and c = 0.583 nm.[18] XRD results indicated that two Bragg peaks were clearly observed in the 2θ region between 4° and 15°. These observed peaks corresponded to lattice spacings d = 1.61 and 0.804 nm. These values are larger than the lattice parameters of $GdNi_4$. The observed phase did not correspond to the $GdNi_4$ phase. Gd_2Ni_7 has a hexagonal Ce_2Ni_7 type (space group $P6_3/mmc$), which is close to the structure of the Sm_5Co_{19} type (space group $P6_3/mmc$). The obtained S, 5.9, of the Ce_2Ni_7-type model was apparently larger than that of the Sm_5Co_{19}-type model. The calculated pattern did not fit well with the observed pattern. The same tendency was also seen in a rhombohedral Gd_2Co_7-type model (space group $R\bar{3}m$); the obtained S was 6.1.

The selected-area electron diffraction (SAED) pattern taken along the ⟨010⟩ direction of Gd_5Ni_{19} is shown in Figure 5, where indexing (100 and 008) of the Sm_5Co_{19}-type structure is given. The high-resolution STEM image of Gd_5Ni_{19} viewed along [100] using a high-angle annular dark field is also shown in Figure 5. Four bright spots along the c-axis direction indicate the Gd atoms, which form a block composed of one layer of $MgZn_2$-type cells and three layers of $CaCu_5$-type cells. These blocks are stacked along the c axis in a sequence of ABAB.... Therefore, the image corresponds to the Sm_5Co_{19}-type structure shown in Figure 3. The Ce_5Co_{19}-type (3R) structure with a stacking sequence of ABCABC... was not observed in the STEM image.

3.2. $P-C$ Isotherm of Gd_5Ni_{19}. The $P-C$ isotherm of Gd_5Ni_{19} at 233 K is shown in Figure 6. In the first absorption process, the maximum hydrogen capacity reached 1.07 H/M at 2.0 MPa. A sloping plateau was observed in the first absorption−desorption process. The plateau pressures of the first absorption and desorption were approximately 0.45 and 0.09 MPa, respectively. After full desorption down to 0.001 MPa in the first cycle, the hydrogen content was 0.26 H/M. Before the second absorption−desorption cycle, the sample was evacuated at 233 K for 3 h. In the second absorption cycle, the maximum hydrogen capacity decreased to 0.87 H/M, while the plateau pressures were the same as those in the first absorption−desorption cycle.

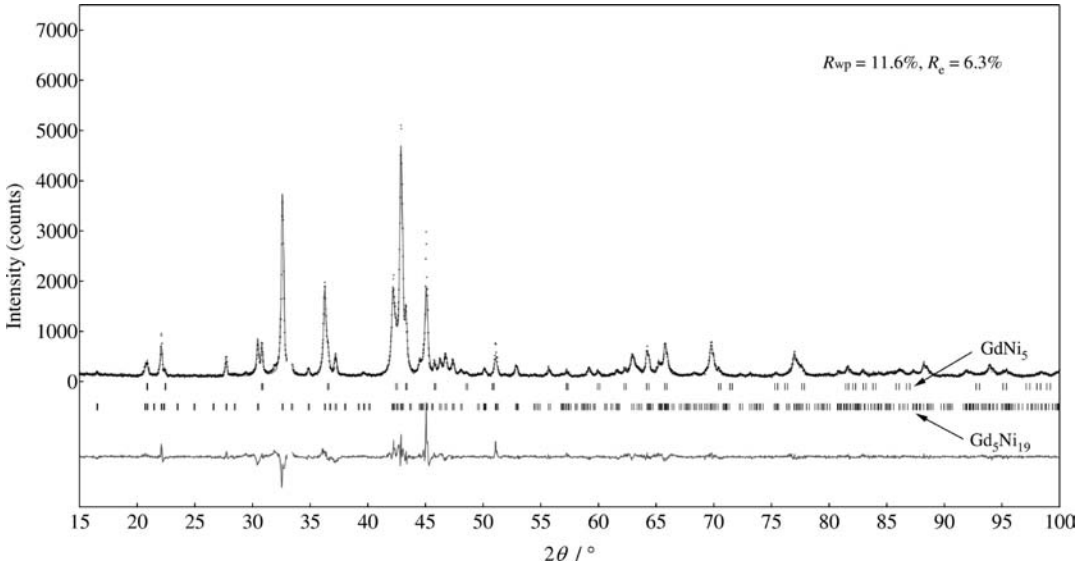

Figure 4. Rietveld refinement of XRD data for the Gd_5Ni_{19} alloy. A model containing Sm_5Co_{19}-type (2H) Gd_5Ni_{19} and $CaCu_5$-type $GdNi_5$ was applied. The line indicates calculated intensities, and the points superimposed on it are the observed intensities. The bottom curve is the difference between the observed and calculated intensities.

dx.doi.org/10.1021/ic201569m |Inorg. Chem. 2011, 50, 11631–11635

Table 1. Structural Parameters of Gd_5Ni_{19} (Space Group $P6_3/mmc$ (No. 194), a = 0.4950(1) nm, c = 3.2161(5) nm, R_{wp} = 11.6%, R_I = 8.8%, R_e = 6.3%, and S = 1.8)

atom	site	g	x	y	z	B (10^{-2} nm^2)
Gd	2c	1.0	$^1/_3$	$^2/_3$	$^1/_4$	0.5(1)
Gd	4f	1.0	$^1/_3$	$^2/_3$	0.1317(1)	1.1(1)
Gd	4f	1.0	$^1/_3$	$^2/_3$	0.0210(1)	1.6(1)
Ni	2a	1.0	0	0	0	1.3(5)
Ni	2b	1.0	0	0	$^1/_4$	0.5(1)
Ni	2d	1.0	$^1/_3$	$^2/_3$	$^3/_4$	0.7(2)
Ni	4e	1.0	0	0	0.1283(2)	0.5(2)
Ni	4f	1.0	$^1/_3$	$^2/_3$	0.8726(2)	0.5(1)
Ni	12k	1.0	0.8326(8)	$2x$	0.0632(1)	0.5(1)
Ni	12k	1.0	0.8331(7)	$2x$	0.1889(1)	0.4(1)

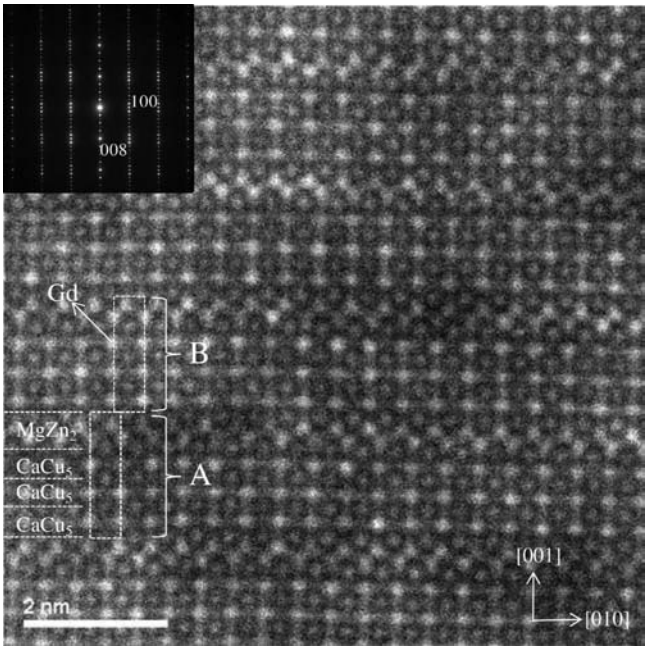

Figure 5. High-resolution STEM image and SAED pattern of Gd_5Ni_{19}.

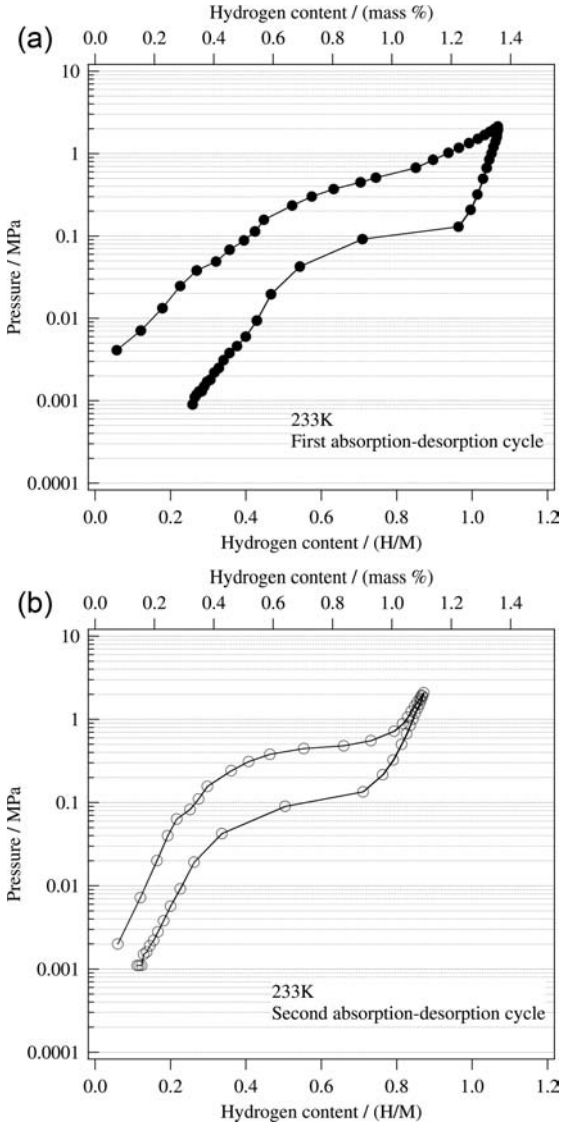

Figure 6. $P-C$ isotherm of Gd_5Ni_{19} at 233 K: (a) first absorption−desorption process; (b) second absorption−desorption process.

4. DISCUSSION

4.1. Crystal Structure. In this study, the heat-treatment condition was fixed to obtain the Gd_5Ni_{19} phase with Sm_5Co_{19}-type structure. As shown in the Gd−Ni phase diagram, Gd_2Ni_7 and $GdNi_4$ are stable below 1473 and 1543 K, respectively. The $GdNi_5$ phase has a melting point at 1753 K, and the phase is stable up to its melting point. The $GdNi_5$ phase increases over 1473 K.

We successfully synthesized the Gd_5Ni_{19} phase. The crystal structure of Gd_5Ni_{19} was investigated by XRD and STEM. The Rietveld refinement of the Sm_5Co_{19}-type model and the Ce_5Co_{19}-type model provided S = 1.8 and 5.5, respectively. A Ce_5Co_{19}-type structure was not observed in either the XRD profile or STEM image. In our study, the crystal structure of Gd_5Ni_{19} was determined to be of the Sm_5Co_{19} type (2H, space group $P6_3/mmc$) with a = 0.4950(1) nm and c = 3.2161(5) nm for the first time. When the lattice parameters of $GdNi_3$, Gd_2Ni_7, and Gd_5Ni_{19} were compared, it was found that a increased with the ratio of Gd_2Ni_4 to $GdNi_5$ cells and was closer to that for the $GdNi_5$ compound. The 001 and 008 spots were clearly observed in the SAED pattern in Figure 5, which satisfied space group $P6_3/mmc$. The result is consistent with the XRD analysis result. Thus, the crystal structure of the synthesized Gd_5Ni_{19} is determined.

Lemort et al. recently reported the synthesis of Pr_5Ni_{19} with Sm_5Co_{19}- and Ce_5Co_{19}-type structures.[11] The lattice parameters of Sm_5Co_{19}-type Pr_5Ni_{19} were a = 0.4999 nm and c = 3.2410 nm. In this study, the lattice parameters of Gd_5Ni_{19} with the Sm_5Co_{19}-type structure were a = 0.4950(1) nm and c = 3.2161(5) nm, which are smaller than those of Pr_5Ni_{19}.

Buschow et al. reported that Pr_2Ni_7 has a hexagonal Ce_2Ni_7-type structure at 1223 K and a stable rhombohedral Gd_2Co_7-type structure at room temperature.[2] They also reported that $PrNi_3$ has a rhombohedral $PuNi_3$-type structure.[2] Gd_2Ni_7 has two types of crystal structures: a hexagonal Ce_2Ni_7-type structure at 873 K and a rhombohedral Gd_2Co_7-type structure at 1173 K.[3] $GdNi_3$ has a rhombohedral $PuNi_3$-type structure like $PrNi_3$. The phase stabilities differ for Pr_2Ni_7 and Gd_2Ni_7. On the other hand, the

dx.doi.org/10.1021/ic201569m |Inorg. Chem. 2011, 50, 11631–11635

crystal structures of $GdNi_3$ and Gd_5Ni_{19} are isomorphic with $PrNi_3$ and Pr_5Ni_{19}.

4.2. Hydrogen Absorption Property. The $P-C$ isotherms of Gd_5Ni_{19} for the first and second absorption−desorption cycles are shown in Figure 6a,b. The maximum hydrogen capacity of the first absorption cycle reached 1.07 H/M. The single sloping plateau was observed in the first absorption−desorption cycle. The same tendency was also seen in the second absorption−desorption cycle, but the maximum hydrogen capacity decreased to 0.87 H/M. This suggests that hydrogen in the amount of H/M = 0.20 remains in the alloy before the second absorption−desorption cycle. The present sample consisted of two phases of 89% Gd_5Ni_{19} and 11% $GdNi_5$ from the Rietveld refinement shown in Figure 4. Senoh et al. reported the $P-C$ isotherm of $GdNi_5$.[6] The initial activation was achieved by a hydrogen gas pressure of 35 MPa at 197 K for several hours. Activation treatment of $GdNi_5$ is not easy. Two plateaus were observed at 223 K: one at 1.5 MPa and the other at 6 MPa. In other words, $GdNi_5$ showed very high plateau pressures. In our results for the $P-C$ isotherm at 233 K, the maximum hydrogen pressure was 2.0 MPa and the plateau pressure was below 1 MPa. Therefore, the obtained $P-C$ isotherm shown in Figure 6 is barely affected by $GdNi_5$.

In our previous study, the crystal structure and $P-C$ isotherm of Pr_5Ni_{19} with the Sm_5Co_{19}-type structure were reported.[19] The crystal structure of Pr_5Ni_{19} was determined by XRD and TEM. The $P-C$ isotherm of the alloy in the first absorption process was clearly different from that in the first desorption process; a single plateau in absorption and three plateaus in desorption were observed. The $P-C$ isotherm of Gd_5Ni_{19} indicated one sloping plateau in both the absorption and desorption processes, which is similar to the trend observed in the isotherm of La_5Ni_{19}. We are interested in the structural changes in the $MgZn_2$- and $CaCu_5$-type cells of Gd_5Ni_{19} during hydrogenation. In order to clarify the structural changes, it is necessary to carry out in situ XRD measurements (neutron diffraction is unsuitable because of the vast absorption cross section of Gd to neutrons).

5. CONCLUSION

We synthesized the intermetallic compound Gd_5Ni_{19} and determined its crystal structure type to be Sm_5Co_{19} (space group $P6_3/mmc$) for the first time. The refined lattice parameters were a = 0.4950(1) nm and c = 3.2161(5) nm. The Rietveld refinement results for the XRD data agreed with the high-resolution STEM analysis results. This phase is stable around 1543 K.

The $P-C$ isotherm of Gd_5Ni_{19} showed a single sloping plateau in both the absorption and desorption processes. The plateau pressure in the first absorption−desorption cycle agreed with that in the second absorption−desorption cycle. The maximum hydrogen capacity of the first absorption cycle reached 1.07 H/M, while that of the second absorption cycle was 0.87 H/M. This means that hydrogen in the amount of H/M = 0.20 remains in the alloy before the second absorption−desorption cycle, even though the sample was evacuated at 233 K for 3 h.

AUTHOR INFORMATION

Corresponding Author

*E-mail: fbiwase@mx.ibaraki.ac.jp. Tel: +81-29-352-3233. Fax: +81-29-287-7189.

ACKNOWLEDGMENT

The authors thank Professor Emeritus H. Asano (University of Tsukuba) for his helpful advice.

REFERENCES

(1) Baenziger, N. C.; Moriarty, J. L., Jr. *Acta Crystallogr.* **1961**, *14*, 948–950.
(2) Buschow, K. H. J.; Van Der Goot, A. S. *J. Less-Common Met.* **1970**, *22*, 419–428.
(3) Virkar, A. V.; Raman, A. *J. Less-Common Met.* **1968**, *18*, 59–66.
(4) Wernick, J. H.; Geller, S. *Acta Crystallogr.* **1959**, *12*, 662–665.
(5) Aoki, K.; Yamamoto, T.; Masumoto, T. *Scr. Met.* **1987**, *21*, 27–31.
(6) Senoh, H.; Takeichi, N.; Takeshita, H. T.; Tanaka, H.; Kiyobayashi, T.; Kuriyama, N. *Mater. Sci. Eng.* **2004**, *B108*, 96–99.
(7) Khan, Y. *Acta Crystallogr.* **1974**, *B30*, 1533–1537.
(8) Yamamoto, T.; Inui, H.; Yamaguchi, M.; Sato, K.; Fujitani, S.; Yonezu, I.; Nishio, K. *Acta Mater.* **1997**, *45*, 5213–5221.
(9) Takeda, S.; Kitano, Y.; Komura, Y. *J. Less-Common Met.* **1982**, *84*, 317–325.
(10) Ferey, A.; Cuevas, F.; Latroche, M.; Knosp, B.; Bernard, P. *Electrochim. Acta* **2009**, *54*, 1710–1714.
(11) Lemort, L.; Latroche, M.; Knosp, B.; Bernard, P. *J. Alloys Compd.* **2011**, in press.
(12) Iwase, K.; Sakaki, K.; Nakamura, Y.; Akiba, E. *Inorg. Chem.* **2010**, *49*, 8763–8768.
(13) Yartys, V. A.; Riabov, A. B.; Denys, R. V.; Sato, M.; Delaplane, R. G. *J. Alloys Compd.* **2006**, *408−412*, 273–279.
(14) *Binary Alloy Phase Diagrams*, 2nd ed. plus updates; Okamoto, H., Ed.; ASM International: Materials Park, OH, 1996.
(15) Izumi, F. http://homepage.mac.com/fujioizumi/.
(16) Izumi, F. *Rigaku J.* **2000**, *17*, 34–45.
(17) Izumi, F.; Young, R. A. *The Rietveld Method*; International Union of Crystallography, Oxford University Press: Oxford, U.K., 1993; p 13.
(18) Novy, V. F.; Vickery, R. C.; Kleber, E. V. *Trans. Metall. Soc. AIME* **1961**, *221*, 585–588.
(19) Iwase, K.; Sakaki, K.; Matsuda, J.; Nakamura, Y.; Ishigaki, T.; Akiba, E. *Inorg. Chem.* **2011**, *50*, 4548–4552.